Journal of Solid Mechanics Vol. 10, No. 4 (2018) pp. 753-765

Dynamic Behavior of Anisotropic Protein Microtubules Immersed in Cytosol Via Cooper–Naghdi Thick Shell Theory

M.R. Ghorbanpour Arani [1,*], Z. Khoddami Maraghi [2], E. Haghparast [2]

[1]*Electrical Engineering Department, Amirkabir University of Technology, Tehran, Iran*
[2]*Faculty of Mechanical Engineering, University of Kashan, Kashan, Iran*

Received 9 July 2018; accepted 14 September 2018

ABSTRACT

In the present research, vibrational behavior of anisotropic protein microtubules (MTs) immersed in cytosol via Cooper–Naghdi shell model is investigated. MTs are hollow cylindrical structures in the eukaryotic cytoskeleton which surrounded by filament network. The temperature effect on vibration frequency is also taken into account by assuming temperature-dependent material properties for MTs. To enhance the accuracy of results, strain gradient theory is utilized and the motion equations are derived based on Hamilton's principle. Effects of various parameters such as environmental conditions by considering the surface traction of cytosol, length scale, thickness and aspect ratio on vibration characteristics of anisotropic MTs are studied. Results indicate that vibrational behavior of anisotropic MTs is strongly dependent on longitudinal Young's modulus and length scale parameters. The results of this investigation can be utilized in the ultrasonic examine of MT organization in medical applications particularly in the treatment of cancers.

Keywords: Anisotropic protein MT; Cooper–Naghdi thick shell model; Strain gradient theory; Visco-elastic bio-medium.

1 INTRODUCTION

INTRACELLULAR fluid (ICF) are named cytosol or cytoplasmic matrix which is a part of cytoplasm in the eukaryotic cell (protists, fungi, plants, animals) . Cell membranes separate cytosol into compartments that one of them is MT. α and β tubulins make up MT in long, hollow cylinder form. Organelles can travel from the center of the cell outward using the tracks that MTs provide. MTs are major components of the cytoskeleton that are responsible for various kinds of movements in all eukaryotic cells and involved in nucleic and cell division [1].

The study of mechanical behaviors of MTs as a branch of biomechanics can help scientists to better understanding of the intracellular environment. In recent years, various researches have been carried out to analyzing of buckling, dynamic stability, flexural rigidity and free vibration of protein MTs. In this regard, Shi et.al [2] utilized Timoshenko beam model to do research about the effect of transverse shearing due to low shear modulus of MT. They founded that the length-dependent flexural rigidity predicted by the Timoshenko beam model have a good agreement with experimental data. Based on the nonlocal Timoshenko beam model, mechanical properties of

*Corresponding author. Tel.: +98 3155912450; Fax: +98 3155912424.
E-mail address: mrezagh6193@gmail.com (M.R.Ghorbanpour Arani).

protein MTs was studied by Gao and Lei [3]. Their results indicate that the small scale parameter plays an important role in the buckling of MTs in living cells. Utilizing parabolic shear deformation theory (PSDT), Tounsi et .al [4] studied vibration and length-dependent flexural rigidity of MT. Their results showed that due to extremely low shear modulus of MTs, the effect of transverse shearing on vibration analysis of MTs must be considered.

Based on modified couple stress theory and TB model, Fu and Zhang [5] studied about mechanical behavior of MT. They proved that increasing the value of material length scale parameter causes to decrease buckling amplitude. Civalek and Demir [6] investigated static response of isotropic MTs based on the nonlocal Euler–Bernoulli beam theory. They concluded that especially for some boundary conditions, the nonlocal continuum theory is superior to local elasticity. In the other work [7], they used nonlocal discrete models to study about torsional and longitudinal frequency and wave response of MTs. Their results showed that size effect must be considered for modelling of MTs particularly for higher modes vibration and phase velocity analysis.

Wang et al. [8] suggested orthotropic elastic shell model for vibrational behavior of MTs. They concluded that vibration frequencies of MTs in isotropic model are estimated higher than orthotropic one at almost vibration modes. Wang and Zhang [9] considered orthotropic shell model to investigate circumferential vibrations of MTs with large axial wavelength. They founded that it cannot be used parabolic dispersion law for circumferential modes. Based on orthotropic Shell-Stokes flow model, Wang et al. [10] identified three kinds of dynamic behavior of MTs in living cells. In addition, they proved that the assumption of ideal fluid surrounding MTs is incorrect. Vibration of MTs due to internal fluid by considering the effect of cytosol and nonlinearity parameter was carried out by Ghorbanpour Arani et al. [11]. They obtained the critical fluid velocity and fluid density in which the dynamic instability of MT occurs.

Effect of transverse shearing on mechanical behavior of orthotropic MTs was presented by Gu et al. [12]. They showed that the accuracy of results for two dimensional (2D) orthotropic shell model is more appropriate than beam-like models when the transverse shearing is considered. By means of anisotropic shell model and Stokes flow theory, Gao and An [13] studied buckling behavior of anisotropic MTs in cytoplasm. Their results indicated that buckling growth rate of MTs is strongly dependent on viscosity of cytosol and small scale parameter. Utilizing first-order shear deformation shell theory, Daneshmand et al. [14] investigated wave propagation in orthotropic MTs. They demonstrated that the shear modules of microtubule have a considerable effect on wave velocities. Dynamic behavior of MT as orthotropic elastic shell embedded in an elastic medium was carried out by Taj and Zhang [15]. They simulated surrounding medium as Pasternak model and showed that increasing Winkler stiffness and shearing layer of surrounding medium cause to increase flexural vibration of MTs. Based on nonlocal shear deformable theory, Shen [16] presented buckling and post buckling of MTs under torsion. Considering properties of anisotropic and temperature-dependent materials for MTs, they founded that temperature changes play a significant role on post buckling of protein MTs subjected to torsion. In the other work, Taj and Zhang [17] performed wave propagation of orthotropic MTs embedded in Pasternak foundation. They demonstrated the effect of surrounding medium on wave velocity of MTs for axisymmetric and non-axisymmetric waves.

Despite mentioned researches, vibration analysis of anisotropic protein MTs based on Cooper-Naghdi shell model and strain gradient shell theory is a novel topic that cannot be found in literatures. Cooper-Naghdi theory is valid for thick shells by considering shear coefficient. Since the MTs are in the nano/micro scale, strain gradient shell theory with three length scale parameters are utilized while the effect of surface, temperature change, surrounded bio-medium, mechanical properties and dimensions are also studied. It seems that simply supported boundary condition is closer to reality according to the initial and final conditions of MTs in the cell. It is hoped to use the results of this study in bio-medical clinical applications.

2 COOPER-NAGHDI THICK SHELL MODEL

In contrast to microfilaments, MTs are thick hollow cylinder made of α and β tubulins. These structures are found throughout the cytoplasm of all eukaryotic cells. Fig.1 illustrates anisotropic MT immersed in cytosol. In this study, MT is considered as a cylindrical tube with equivalent thickness h. Also, MT is simulated by thick shell model to achieve more accuracy.

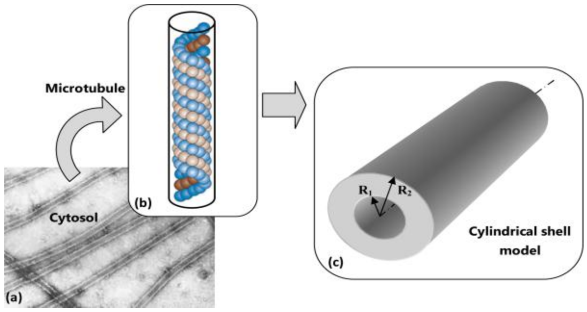

Fig.1
Modelling of MTs: a) Mmicroscopic images of MTs immersed in cytosol in a cell. b) The schematic of MT composed of tubulins. c) Cylindrical thick shell to modelling of MT.

According to Cooper-Naghdi thick shell model, the displacement components of cylindrical shell in the axial x, circumferential θ, and radial z directions can be written as [18]:

$$\begin{aligned}\tilde{U}(x,\theta,z,t) &= u(x,\theta,t) + z\,\beta_x(x,\theta,t),\\ \tilde{V}(x,\theta,z,t) &= v(x,\theta,t) + z\,\beta_\theta(x,\theta,t),\\ \tilde{W}(x,\theta,z,t) &= w(x,\theta,t),\end{aligned} \tag{1}$$

where β_x and β_θ represent axial and circumferential shear effects. z is the distance from an arbitrary point to the middle surface. u, v and w denote the displacement components of the middle surface of the shell in the axial, circumferential and radial directions, respectively. Therefore, strain-displacement relationships can be written as [18]:

$$\begin{aligned}\varepsilon_{xx} &= \frac{\partial u}{\partial x} + z\frac{\partial \beta_x}{\partial x},\\ \varepsilon_{\theta\theta} &= \frac{1}{R}\frac{\partial v}{\partial \theta} + \frac{z}{R}\frac{\partial \beta_\theta}{\partial \theta},\\ \varepsilon_{x\theta} &= \frac{1}{2}\frac{\partial v}{\partial x} + \frac{z}{2}\frac{\partial \beta_\theta}{\partial x} + \frac{1}{2R}\frac{\partial u}{\partial \theta} + \frac{z}{2R}\frac{\partial \beta_x}{\partial \theta},\\ \varepsilon_{xz} &= \frac{1}{2}\frac{\partial w}{\partial x} + \frac{1}{2}\beta_x,\\ \varepsilon_{\theta z} &= \frac{1}{2R}\frac{\partial w}{\partial \theta} + \frac{1}{2}\beta_\theta.\end{aligned} \tag{2}$$

Recently, many experimental tests have been performed to obtain the physical and mechanical properties of MTs in living cells. It has been proved that longitudinal Young's modulus is higher than shear modulus and circumferential Young's modulus of MTs. It's due to stronger bond between $\alpha-\beta$ dimmers along the MTs than lateral bond between adjacent filaments [14]. Consequently, anisotropic thick shell is the real model to simulate protein MTs accurately. Therefore, MTs are assumed anisotropic with E_x and E_y as a Young's moduli in the longitudinal and circumferential directions, respectively. G_{xz} and G_{yz}, are transverse shear moduli and G_{xy} is in-plane shear modulus. υ_x and $\upsilon_\theta = \upsilon_x (E_\theta / E_x)$ are poisson's ratios along the axial and circumferential directions of MTs.

Assuming plane strain condition, the constitutive equations for anisotropic MTs are expressed as [19]:

$$\begin{Bmatrix}\sigma_{xx}\\ \sigma_{\theta\theta}\\ \tau_{\theta z}\\ \tau_{xz}\\ \tau_{x\theta}\end{Bmatrix} = [Q]\begin{Bmatrix}\varepsilon_{xx}\\ \varepsilon_{\theta\theta}\\ \varepsilon_{\theta z}\\ \varepsilon_{xz}\\ \varepsilon_{x\theta}\end{Bmatrix}, \tag{3}$$

where Q is the stiffness matrix which is defined as [14]:

$$[Q]=\begin{bmatrix} \frac{E_x}{1-\upsilon_x\,\upsilon_\theta} & \frac{\upsilon_\theta\,E_x}{1-\upsilon_x\,\upsilon_\theta} & 0 & 0 & 0 \\ \frac{\upsilon_\theta\,E_x}{1-\upsilon_x\,\upsilon_\theta} & \frac{E_\theta}{1-\upsilon_x\,\upsilon_\theta} & 0 & 0 & 0 \\ 0 & 0 & \frac{K.G_{\theta z}}{2} & 0 & 0 \\ 0 & 0 & 0 & \frac{K.G_{xz}}{2} & 0 \\ 0 & 0 & 0 & 0 & \frac{G_{x\theta}}{2} \end{bmatrix}, \tag{4}$$

where K is the shear coefficient. Based on Reissner's variational theorem [20] the value of this coefficient is chosen 5/6.

3 STRAIN GRADIENT SHELL THEORY (SGST)

Based on strain gradient theory, the strain energy U is dependent on higher-order stresses as follows [21]:

$$\begin{aligned} U &= \frac{1}{2}\int_\Omega (\sigma_{ij}\,\varepsilon_{jk} + p_i\,\gamma_i + \tau^{(1)}_{ijk}\eta^{(1)}_{ijk} + m_{ij}\,\chi_{ij})dV \\ &= \frac{1}{2}\int_0^{2\pi}\int_0^{L}\int_{-h_i/2}^{h_i/2} (\sigma_{xx}\,\varepsilon_{xx} + \sigma_{\theta\theta}\varepsilon_{\theta\theta} + 2\tau_{x\theta}\varepsilon_{x\theta} + 2\tau_{xz}\,\varepsilon_{xz} + 2\tau_{z\theta}\varepsilon_{z\theta} + p_i\,\gamma_i + \tau^{(1)}_{ijk}\eta^{(1)}_{ijk} + m_{ij}\,\chi_{ij})\,R\,dz\,dx\,d\theta, \end{aligned} \tag{5}$$

where $\eta^{(1)}_{ijk}$, χ_{ij} and γ_i denote the deviatoric stretch gradient, dilatation and symmetric rotation gradient tensors ,respectively, which are defined as [21]:

$$\eta^{(1)}_{ijk} = \frac{1}{3}\left(\frac{\partial\varepsilon_{jk}}{\partial x_i} + \frac{\partial\varepsilon_{ki}}{\partial x_j} + \frac{\partial\varepsilon_{ij}}{\partial x_k}\right) - \frac{1}{15}\left[\delta_{ij}\,(\frac{\partial\varepsilon_{mm}}{\partial x_k} + 2\frac{\partial\varepsilon_{mk}}{\partial x_m}) + \delta_{jk}\,(\frac{\partial\varepsilon_{mm}}{\partial x_i} + 2\frac{\partial\varepsilon_{mi}}{\partial x_m}) + \delta_{ki}\,(\frac{\partial\varepsilon_{mm}}{\partial x_j} + 2\frac{\partial\varepsilon_{mj}}{\partial x_m})\right],$$

$$\begin{cases} \eta^{(1)}_{x\theta z} = \eta^{(1)}_{\theta zx} = \eta^{(1)}_{zx\theta} = \eta^{(1)}_{z\theta x} = \eta^{(1)}_{xz\theta} = \eta^{(1)}_{\theta xz} = \frac{1}{3}\left(\frac{\partial\varepsilon_{\theta z}}{\partial x} + \frac{1}{R}\frac{\partial\varepsilon_{zx}}{\partial\theta} + \frac{\partial\varepsilon_{x\theta}}{\partial z}\right), \\ \eta^{(1)}_{xxx} = \frac{\partial\varepsilon_{xx}}{\partial x} - \frac{1}{5}\left[\frac{\partial\varepsilon_{xx}}{\partial x} + \frac{\partial\varepsilon_{\theta\theta}}{\partial x} + 2\frac{\partial\varepsilon_{xx}}{\partial x} + \frac{2}{R}\frac{\partial\varepsilon_{\theta x}}{\partial\theta}\right], \\ \eta^{(1)}_{\theta\theta\theta} = \frac{1}{R}\frac{\partial\varepsilon_{\theta\theta}}{\partial\theta} - \frac{1}{5}\left[\frac{1}{R}\frac{\partial\varepsilon_{xx}}{\partial\theta} + \frac{1}{R}\frac{\partial\varepsilon_{\theta\theta}}{\partial\theta} + 2\frac{\partial\varepsilon_{x\theta}}{\partial x} + \frac{2}{R}\frac{\partial\varepsilon_{\theta\theta}}{\partial\theta}\right], \\ \eta^{(1)}_{xx\theta} = \eta^{(1)}_{\theta xx} = \eta^{(1)}_{x\theta x} = \frac{1}{3}\left(\frac{2\partial\varepsilon_{x\theta}}{\partial x} + \frac{1}{R}\frac{\partial\varepsilon_{xx}}{\partial\theta}\right) - \frac{1}{15}\left[\frac{1}{R}\frac{\partial\varepsilon_{xx}}{\partial\theta} + \frac{1}{R}\frac{\partial\varepsilon_{\theta\theta}}{\partial\theta} + 2\frac{\partial\varepsilon_{x\theta}}{\partial x} + \frac{2}{R}\frac{\partial\varepsilon_{\theta\theta}}{\partial\theta}\right], \\ \eta^{(1)}_{x\theta\theta} = \eta^{(1)}_{\theta x\theta} = \eta^{(1)}_{\theta\theta x} = \frac{1}{3}\left(\frac{2}{R}\frac{\partial\varepsilon_{x\theta}}{\partial\theta} + \frac{\partial\varepsilon_{\theta\theta}}{\partial x}\right) - \frac{1}{15}\left[\frac{\partial\varepsilon_{xx}}{\partial x} + \frac{\partial\varepsilon_{\theta\theta}}{\partial x} + \frac{2}{R}\frac{\partial\varepsilon_{x\theta}}{\partial\theta} + 2\frac{\partial\varepsilon_{xx}}{\partial x}\right], \\ \eta^{(1)}_{zzz} = -\frac{1}{5}\left[\frac{\partial\varepsilon_{xx}}{\partial z} + \frac{\partial\varepsilon_{\theta\theta}}{\partial z}\right], \\ \eta^{(1)}_{xzz} = \eta^{(1)}_{zxz} = \eta^{(1)}_{zzx} = -\frac{1}{15}\left[\frac{\partial\varepsilon_{xx}}{\partial x} + \frac{\partial\varepsilon_{\theta\theta}}{\partial x} + \frac{2}{R}\frac{\partial\varepsilon_{x\theta}}{\partial\theta} + 2\frac{\partial\varepsilon_{xx}}{\partial x}\right], \\ \eta^{(1)}_{\theta zz} = \eta^{(1)}_{z\theta z} = \eta^{(1)}_{zz\theta} = -\frac{1}{15}\left[\frac{1}{R}\frac{\partial\varepsilon_{xx}}{\partial\theta} + \frac{1}{R}\frac{\partial\varepsilon_{\theta\theta}}{\partial\theta} + 2\frac{\partial\varepsilon_{x\theta}}{\partial x} + \frac{2}{R}\frac{\partial\varepsilon_{\theta\theta}}{\partial\theta}\right], \\ \eta^{(1)}_{z\theta\theta} = \eta^{(1)}_{\theta z\theta} = \eta^{(1)}_{\theta\theta z} = \frac{1}{3}\left(\frac{\partial\varepsilon_{\theta\theta}}{\partial z}\right) - \frac{1}{15}\left[\frac{\partial\varepsilon_{xx}}{\partial z} + \frac{\partial\varepsilon_{\theta\theta}}{\partial z}\right], \\ \eta^{(1)}_{xxz} = \eta^{(1)}_{zxx} = \eta^{(1)}_{xzx} = \frac{1}{3}\left(\frac{\partial\varepsilon_{xx}}{\partial z}\right) - \frac{1}{15}\left[\frac{\partial\varepsilon_{xx}}{\partial z} + \frac{\partial\varepsilon_{\theta\theta}}{\partial z}\right], \end{cases} \tag{6a}$$

$$\gamma_i = \frac{\partial \varepsilon_{mm}}{\partial x_i},$$

$$\begin{cases} \gamma_x = \dfrac{\partial \varepsilon_{xx}}{\partial x} + \dfrac{\partial \varepsilon_{\theta\theta}}{\partial x}, \\ \gamma_\theta = \dfrac{1}{R}\dfrac{\partial \varepsilon_{xx}}{\partial \theta} + \dfrac{1}{R}\dfrac{\partial \varepsilon_{\theta\theta}}{\partial \theta}, \\ \gamma_z = \dfrac{\partial \varepsilon_{xx}}{\partial z} + \dfrac{\partial \varepsilon_{\theta\theta}}{\partial z}. \end{cases} \tag{6b}$$

$$\chi_{ij} = \frac{1}{2}\left(e_{ipq}\frac{\partial \varepsilon_{qj}}{\partial x_p} + e_{jpq}\frac{\partial \varepsilon_{qi}}{\partial x_p} \right),$$

$$\begin{cases} \chi_{x\theta} = \chi_{\theta x} = \dfrac{1}{2}\left[\dfrac{\partial \varepsilon_{x\theta}}{\partial z} + \dfrac{\partial \varepsilon_{xx}}{\partial z} - \dfrac{\partial \varepsilon_{\theta\theta}}{\partial z} \right], \\ \chi_{\theta\theta} = \dfrac{\partial \varepsilon_{x\theta}}{\partial z}, \\ \chi_{xx} = -\dfrac{\partial \varepsilon_{x\theta}}{\partial z}, \\ \chi_{zz} = 0, \\ \chi_{xz} = \chi_{zx} = \dfrac{1}{2}\left[\dfrac{\partial \varepsilon_{x\theta}}{\partial x} - \dfrac{1}{R}\dfrac{\partial \varepsilon_{xx}}{\partial \theta} \right], \\ \chi_{\theta z} = \chi_{z\theta} = \dfrac{1}{2}\left[\dfrac{\partial \varepsilon_{\theta\theta}}{\partial x} - \dfrac{1}{R}\dfrac{\partial \varepsilon_{x\theta}}{\partial \theta} \right], \end{cases} \tag{6c}$$

where δ_{ij}, e_{jpq} are Kronecker delta and alternate tensor, respectively. The higher-order stresses p_i, $\tau_{ijk}^{(1)}$ and m_{ij} are given by [21]:

$$p_i = 2l_0^2 G\gamma_i, \tag{7a}$$

$$\tau_{ijk}^{(1)} = 2l_1^2 G\eta_{ijk}^{(1)}, \tag{7b}$$

$$m_{ij} = 2l_2^2 G\chi_{ij}, \tag{7c}$$

where G is the shear modulus. Also l_0, l_1 and l_2 are independent material length scale parameters. It is worth to mention that in-plane and transverse shear modules of MTs have almost identical values ($G_{xz} = G_{yz} = G_{xy}$) according to Ref. [14].

4 KINETIC ENERGY

The kinetic energy of the anisotropic MT can be expressed as [22]:

$$K_{MT} = \frac{\rho_m A}{2}\int_0^L \left[\left(\frac{\partial \tilde{U}}{\partial t}\right)^2 + \left(\frac{\partial \tilde{V}}{\partial t}\right)^2 + \left(\frac{\partial \tilde{W}}{\partial t}\right)^2 \right] dx, \tag{8}$$

where ρ_m is the mass density of MT.

5 SIMULATION OF SURROUNDING BIO-MEDIUM

The lateral force applied on MTs due to visco-elastic surrounding bio-medium is expressed as [23]:

$$F = F_s + F_f, \tag{9}$$

where F_s and F_f are the lateral surface traction and the produced force due to filament network, respectively, which are defined as [23]:

$$F_s = \pi\mu\eta\frac{\partial w}{\partial t} \quad where \quad \eta = \frac{(1-q^4)\ln q - 12q^2 + 2q^4 + 10}{(q^4-1)\ln q + 2q^2 - q^4 - 1} \quad q = \frac{R_2}{R_1}, \tag{10a}$$

$$F_f = \chi w \quad where \quad \chi = 2.7E_c, \tag{10b}$$

where E_c and μ are the elastic modulus and viscosity of surrounding bio-medium [23].

The external work due to surrounding bio-medium can be written as:

$$\Omega_{medium} = \frac{1}{2}\int_0^{2\pi}\int_0^{L} F\, W dx\, R d\theta \tag{11}$$

6 SURFACE ENERGY

The surface energy in nano-scale is considered using two distinct effects [24, 25, 26].

The first effect is on bending rigidity. EI must be changed to $E_e I_e$ in the motion equations as follows:

$$E_e I_e = EI + h, \quad h = \pi E_s t_0 (R_1^3 + R_2^3), \tag{12}$$

where E_s, t_0 are Young's modulus and thickness of surface layers, respectively.

The second effect is known as surface residual stress. According to Laplace–Young equation, the transverse loading exerted on the MT due to surface residual tension is defined as:

$$q(x,t) = H\frac{\partial^2 w(x,t)}{\partial x^2}, \quad H = 4\tau_0(R_1 + R_2), \tag{13}$$

where τ_0 is the residual surface tension.

Surface effects on the mechanical behavior of MTs can be described using above relations.

7 MOTION EQUATIONS

According to Hamilton's principle ($\delta\int_{t_1}^{t_2}[K - (U - \Omega_{medium})]dt = 0$) the variational form of the motion equations can be obtained for $\delta u, \delta v, \delta w, \delta\beta_x, \delta\beta_\theta$. In order to summarize relations, the dimensionless parameters for MTs can be introduced as:

$$
\begin{gathered}
(\bar{u},\bar{v},\bar{w})=\frac{(u,v,w)}{R}\qquad \zeta=\frac{x}{L}\qquad \alpha_0=\frac{l_0^{\,2}}{L^2}\qquad \alpha_1=\frac{l_1^{\,2}}{L^2}\qquad \alpha_2=\frac{l_2^{\,2}}{L^2}\qquad \beta=\frac{L}{R}\qquad \bar{h}=\frac{h}{L}\\
\tau=\frac{t}{L}\sqrt{\frac{G_{x\theta}}{\rho_m}}\qquad \bar{Q}_{ij}=\frac{Q_{ij}}{G_{x\theta}}\qquad \bar{\mu}=\frac{\mu}{2\sqrt{\rho_m G_{x\theta}h}}\qquad S=\frac{\chi}{G_{x\theta}}\qquad X=\frac{L}{2\pi h}\qquad \gamma=\frac{G_{x\theta}}{E_x}=\frac{G_{xz}}{E_x}=\frac{G_{\theta z}}{E_x}
\end{gathered}
\tag{14}
$$

Applying Hamilton's principle on Eqs. (5), (8) and (11), the dimensionless motion equations for Cooper-Naghdi thick shell model are obtained as follows:

$$
\begin{aligned}
&-\frac{1}{4}Q_{66}\frac{\partial^2 v}{\partial\xi^2}-\frac{4}{5}\alpha_1\beta^2\frac{\partial^4 v}{\partial\xi^2\partial\theta^2}-\frac{2}{5}\alpha_1\beta^2\frac{\partial^4 u}{\partial\xi^3\partial\theta}+\frac{4}{15}\alpha_1\beta^3\frac{\partial^4 u}{\partial\xi\partial\theta^3}+\frac{1}{4}\alpha_2\beta\frac{\partial^4 u}{\partial\xi^3\partial\theta}+\alpha_2\beta^2\frac{\partial^4 v}{\partial\xi^2\partial\theta^2}+\frac{16}{15}\alpha_1\beta^2\frac{\partial^4 v}{\partial\xi^2\partial\theta^2}\\
&-\frac{1}{2}\alpha_2\beta\frac{\partial^4 u}{\partial\xi^3\partial\theta}-\alpha_2\beta^2\frac{\partial^4 v}{\partial\xi^2\partial\theta^2}+2\alpha_0\beta^4\frac{\partial^4 v}{\partial\theta^4}+2\alpha_0\beta^2\frac{\partial^4 v}{\partial\xi^2\partial\theta^2}-\frac{2}{5}\alpha_1\beta\frac{\partial^4 u}{\partial\xi^3\partial\theta}+\frac{4}{5}\alpha_1\beta^4\frac{\partial^4 v}{\partial\theta^4}+\frac{8}{15}\alpha_1\beta^2\frac{\partial^4 v}{\partial\xi^2\partial\theta^2}\\
&+\frac{8}{15}\alpha_1\beta\frac{\partial^4 u}{\partial\xi^3\partial\theta}+\frac{1}{4}\alpha_2\frac{\partial^4 v}{\partial\xi^4}+\frac{1}{4}\alpha_2\beta^2\frac{\partial^4 v}{\partial\xi^2\partial\theta^2}-Q_{22}\beta^2\frac{\partial^2 v}{\partial\theta^2}-\frac{1}{2}Q_{12}\beta\frac{\partial^2 u}{\partial\xi\partial\theta}-\frac{1}{2}Q_{21}\beta\frac{\partial^2 u}{\partial\xi\partial\theta}-\frac{1}{4}Q_{66}\beta\frac{\partial^2 u}{\partial\xi\partial\theta}+\frac{8}{15}\alpha_1\frac{\partial^4 v}{\partial\xi^4}\\
&+\frac{8}{15}\alpha_1\beta^2\frac{\partial^4 v}{\partial\xi^2\partial\theta^2}+\frac{8}{15}\alpha_1\beta\frac{\partial^4 u}{\partial\xi^3\partial\theta}+2\alpha_0\beta^3\frac{\partial^4 u}{\partial\xi\partial\theta^3}+2\alpha_0\beta\frac{\partial^4 u}{\partial\xi^3\partial\theta}+\frac{1}{4}\alpha_2\beta_0^{\,3}\frac{\partial^4 u}{\partial\xi\partial\theta^3}-\frac{1}{2}\alpha_2\beta^3\frac{\partial^4 u}{\partial\xi\partial\theta^3}-\frac{\partial^2 v}{\partial\tau^2}=0
\end{aligned}
\tag{15a}
$$

$$
\begin{aligned}
&-Q_{11}\frac{\partial^2 u}{\partial\xi^2}-\frac{4}{5}\alpha_1\beta^2\frac{\partial^4 u}{\partial\xi^2\partial\theta^2}-\frac{2}{5}\alpha_1\beta^2\frac{\partial^4 v}{\partial\xi^3\partial\theta}+\frac{4}{15}\alpha_1\beta^3\frac{\partial^4 v}{\partial\xi\partial\theta^3}+\frac{1}{4}\alpha_2\beta\frac{\partial^4 v}{\partial\xi^3\partial\theta}+\frac{8}{15}\alpha_1\beta^2\frac{\partial^4 u}{\partial\xi^2\partial\theta^2}+\frac{8}{15}\alpha_1\beta^4\frac{\partial^4 u}{\partial\theta^4}\\
&+\frac{16}{15}\alpha_1\beta^2\frac{\partial^4 u}{\partial\xi^2\partial\theta^2}-\frac{1}{2}\alpha_2\beta\frac{\partial^4 v}{\partial\xi^3\partial\theta}-\alpha_2\beta^2\frac{\partial^4 u}{\partial\xi^2\partial\theta^2}+\frac{1}{4}\alpha_2\beta^4\frac{\partial^4 u}{\partial\theta^4}+\frac{1}{4}\alpha_2\beta^2\frac{\partial^4 u}{\partial\xi^2\partial\theta^2}+2\alpha_0\beta^2\frac{\partial^4 u}{\partial\xi^2\partial\theta^2}-\frac{2}{5}\alpha_1\beta\frac{\partial^4 v}{\partial\xi^3\partial\theta}\\
&+\frac{8}{15}\alpha_1\beta^2\frac{\partial^4 v}{\partial\xi^3\partial\theta}+\alpha_2\beta^2\frac{\partial^4 u}{\partial\xi^2\partial\theta^2}+2\alpha_0\frac{\partial^4 u}{\partial\xi^4}-\frac{1}{4}Q_{66}\beta^2\frac{\partial^2 u}{\partial\theta^2}-\frac{1}{2}Q_{12}\beta\frac{\partial^2 v}{\partial\xi\partial\theta}-\frac{1}{2}Q_{21}\beta\frac{\partial^2 v}{\partial\xi\partial\theta}-\frac{1}{4}Q_{66}\beta\frac{\partial^2 v}{\partial\xi\partial\theta}\\
&+\frac{4}{5}\alpha_1\frac{\partial^4 u}{\partial\xi^4}+\frac{8}{15}\alpha_1\beta^2\frac{\partial^4 u}{\partial\xi^2\partial\theta^2}+\frac{8}{15}\alpha_1\beta\frac{\partial^4 v}{\partial\xi^3\partial\theta}+2\alpha_0\beta^3\frac{\partial^4 v}{\partial\xi\partial\theta^3}+2\alpha_0\beta\frac{\partial^4 v}{\partial\xi^3\partial\theta}+\frac{1}{4}\alpha_2\beta^3\frac{\partial^4 v}{\partial\xi\partial\theta^3}-\frac{1}{2}\alpha_2\beta^3\frac{\partial^4 v}{\partial\xi\partial\theta^3}-\frac{\partial^2 u}{\partial\tau^2}=0
\end{aligned}
\tag{15b}
$$

$$
\begin{aligned}
&-\frac{1}{4}Q_{55}\frac{\partial^2 w}{\partial\xi^2}+\frac{2}{5}\alpha_1\beta^2\frac{\partial^3\beta_x}{\partial\xi\partial\theta^2}+\frac{8}{15}\alpha_1\beta^2\frac{\partial^3\beta_\theta}{\partial\xi^2\partial\theta}+\frac{1}{3}\alpha_1\beta^2\frac{\partial^3\beta_x}{\partial\xi\partial\theta^2}-\frac{1}{4}\alpha_2\frac{\partial^3\beta_x}{\partial\xi^3}-\frac{5}{4}\alpha_2\beta^2\frac{\partial^3\beta_\theta}{\partial\xi^2\partial\theta}+\alpha_2\beta^2\frac{\partial^3\beta_x}{\partial\xi\partial\theta^2}\\
&+\frac{1}{4}\alpha_2\beta^3\frac{\partial^3\beta_\theta}{\partial\theta^3}-\frac{1}{2}\alpha_2\beta^2\frac{\partial^4 w}{\partial\xi^2\partial\theta^2}+\frac{1}{4}\alpha_2\beta^4\frac{\partial^4 w}{\partial\theta^4}+\alpha_1\beta^2\frac{\partial^4 w}{\partial\xi^2\partial\theta^2}+\frac{2}{3}\alpha_1\beta\frac{\partial^3\beta_\theta}{\partial\xi^2\partial\theta}+\frac{1}{3}\alpha_1\beta^2\frac{\partial^3\beta_x}{\partial\xi\partial\theta^2}+\frac{16}{15}\alpha_1\frac{\partial^3\beta_x}{\partial\xi^3}\\
&-\frac{2}{15}\alpha_1\beta\frac{\partial^3\beta_\theta}{\partial\xi^2\partial\theta}+\frac{8}{15}\alpha_1\beta^4\frac{\partial^4 w}{\partial\theta^4}+\alpha_2\beta^2\frac{\partial^4 w}{\partial\xi^2\partial\theta^2}+\frac{1}{4}\alpha_2\frac{\partial^4 w}{\partial\xi^4}-\frac{1}{4}Q_{55}\frac{\partial\beta_x}{\partial\xi}-\frac{1}{4}Q_{44}\beta^2\frac{\partial^2 w}{\partial\theta^2}-\frac{1}{4}Q_{44}\beta\frac{\partial\beta_\theta}{\partial\theta}\\
&+\frac{1}{3}\alpha_1\beta^2\frac{\partial^4 w}{\partial\xi^2\partial\theta^2}+\frac{16}{15}\alpha_1\beta^3\frac{\partial^3\beta_\theta}{\partial\theta^3}-\frac{4}{15}\alpha_1\beta^2\frac{\partial^4 w}{\partial\xi^2\partial\theta^2}-\frac{1}{2}\alpha_2\beta^2\frac{\partial^3\beta_x}{\partial\xi\partial\theta^2}+\alpha_2\beta\frac{\partial^3\beta_\theta}{\partial\xi^2\partial\theta}-\frac{3}{4}\alpha_2\beta^2\frac{\partial^3\beta_x}{\partial\xi\partial\theta^2}\\
&-\frac{1}{2}\alpha_2\beta^3\frac{\partial^3\beta_\theta}{\partial\theta^3}-SX\beta w-\eta\bar{\mu}\beta\frac{\partial w}{\partial\tau}-\frac{\partial^2 w}{\partial\tau^2}=0
\end{aligned}
\tag{15c}
$$

$$
\begin{aligned}
&2\alpha_0\beta^3\frac{\partial^4\beta_\theta}{\partial\xi\partial\theta^3}+2\alpha_0\beta\frac{\partial^4\beta_\theta}{\partial\xi^3\partial\theta}+\frac{1}{4}\alpha_2\beta^3\frac{\partial^4\beta_\theta}{\partial\xi^3\partial\theta}+\frac{1}{4}\alpha_2\beta^3\frac{\partial^4\beta_\theta}{\partial\xi\partial\theta^3}-\frac{1}{2}\alpha_2\beta^3\frac{\partial^4\beta_\theta}{\partial\xi\partial\theta^3}-\frac{4}{5}\alpha_1\beta^2\frac{\partial^4\beta_x}{\partial\xi^2\partial\theta^2}\\
&-\frac{2}{5}\alpha_1\beta^3\frac{\partial^4\beta_\theta}{\partial\xi\partial\theta^3}-\frac{2}{5}\alpha_1\beta^3\frac{\partial^4\beta_\theta}{\partial\xi\partial\theta^3}+\frac{8}{15}\alpha_1\beta\frac{\partial^4\beta_\theta}{\partial\xi^3\partial\theta}+\frac{1}{4}\alpha_2\beta^4\frac{\partial^4\beta_x}{\partial\theta^4}+\frac{16}{15}\alpha_1\beta^2\frac{\partial^4\beta_x}{\partial\xi^2\partial\theta^2}+\frac{8}{15}\alpha_1\beta^4\frac{\partial^4\beta_x}{\partial\theta^4}\\
&-\frac{128}{5}\frac{\alpha_1}{h^2}\frac{\partial^2\beta_x}{\partial\xi^2}-4\frac{\alpha_1}{h^2}\beta^2\frac{\partial^2\beta_x}{\partial\theta^2}+3\frac{Q_{55}}{h^2}\beta_x+\frac{2}{15}\alpha_1\beta\frac{\partial^4\beta_\theta}{\partial\xi^3\partial\theta}+\frac{8}{15}\alpha_1\beta^3\frac{\partial^4\beta_\theta}{\partial\xi\partial\theta^3}+\frac{8}{15}\alpha_1\beta^3\frac{\partial^4\beta_\theta}{\partial\xi\partial\theta^3}\\
&-\frac{2}{5}\alpha_1\beta\frac{\partial^4\beta_\theta}{\partial\xi^3\partial\theta}+\frac{1}{4}\alpha_2\beta^2\frac{\partial^4\beta_x}{\partial\xi^2\partial\theta^2}+\frac{8}{15}\alpha_1\beta^2\frac{\partial^4\beta_x}{\partial\xi^2\partial\theta^2}+2\alpha_0\beta^2\frac{\partial^4\beta_x}{\partial\xi^2\partial\theta^2}-\alpha_2\beta^2\frac{\partial^4\beta_x}{\partial\xi^2\partial\theta^2}\\
&-\frac{1}{2}Q_{21}\beta\frac{\partial^2\beta_\theta}{\partial\xi\partial\theta}-\frac{1}{4}Q_{66}\beta\frac{\partial^2\beta_\theta}{\partial\xi\partial\theta}-\frac{1}{2}\alpha_2\beta\frac{\partial^4\beta_\theta}{\partial\xi^3\partial\theta}-\frac{24}{5}\frac{\alpha_1\beta^2}{h^2}\frac{\partial^3 w}{\partial\xi\partial\theta^2}-4\frac{\alpha_1}{h^2}\beta^2\frac{\partial^3 w}{\partial\xi\partial\theta^2}-\frac{1}{2}Q_{12}\beta\frac{\partial^2\beta_\theta}{\partial\xi\partial\theta}\\
&+3\frac{\alpha_2}{\beta h^2}\frac{\partial^3 w}{\partial\xi^3}-12\frac{\alpha_2\beta^2}{h^2}\frac{\partial^3 w}{\partial\xi\partial\theta^2}-\frac{1}{4}Q_{66}\beta^2\frac{\partial^2\beta_x}{\partial\theta^2}-\frac{24}{5}\frac{\alpha_1\beta}{h^2}\frac{\partial^2\beta_\theta}{\partial\xi\partial\theta}-24\frac{\alpha_0}{h^2}\beta.\frac{\partial^2\beta_\theta}{\partial\xi\partial\theta}-Q_{11}\frac{\partial^2\beta_x}{\partial\xi^2}
\end{aligned}
\tag{15d}
$$

$$+2\alpha_0\frac{\partial^4\beta_x}{\partial\xi^4}+\frac{8}{15}\alpha_1\beta^2\frac{\partial^4\beta_\theta}{\partial\xi^2\partial\theta^2}+\frac{4}{5}\alpha_1\frac{\partial^4\beta_x}{\partial\xi^4}+\alpha_2\beta^2\frac{\partial^4\beta_x}{\partial\xi^2\partial\theta^2}-\frac{24}{5}\frac{\alpha_1\beta}{h^2}\frac{\partial^2\beta_\theta}{\partial\xi\partial\theta}-4\frac{\alpha_1}{h^2}\beta^2\frac{\partial^2\beta_x}{\partial\theta^2}$$
$$-8\frac{\alpha_1}{h^2}\beta^2\frac{\partial^2\beta_x}{\partial\theta^2}-4\frac{\alpha_1}{h^2}\beta^2\frac{\partial^3 w}{\partial\xi\partial\theta^2}-\frac{64}{5}\frac{\alpha_1}{\beta h^2}\frac{\partial^3 w}{\partial\xi^3}-3\frac{\alpha_2}{h^2}\frac{\partial^2\beta_x}{\partial\xi^2}-12\frac{\alpha_2}{h^2}\beta^2\frac{\partial^2\beta_x}{\partial\theta^2}-24\frac{\alpha_0}{h^2}\frac{\partial^2\beta_x}{\partial\xi^2} \quad (15d)$$
$$+9\frac{\alpha_2\beta}{h^2}\frac{\partial^2\beta_\theta}{\partial\xi\partial\theta}+15\frac{\alpha_2\beta^2}{h^2}\frac{\partial^3 w}{\partial\xi\partial\theta^2}-\frac{\partial^2\beta_x}{\partial\tau^2}=0$$

$$2\alpha_0\beta^3\frac{\partial^4\beta_x}{\partial\xi\partial\theta^3}+2\alpha_0\beta\frac{\partial^4\beta_x}{\partial\xi^3\partial\theta}+\frac{1}{4}\alpha_2\beta^3\frac{\partial^4\beta_x}{\partial\xi^3\partial\theta}+\frac{1}{4}\alpha_2\beta^3\frac{\partial^4\beta x}{\partial\xi\partial\theta^3}-\frac{1}{2}\alpha_2\beta^3\frac{\partial^4\beta_x}{\partial\xi\partial\theta^3}-\frac{4}{5}\alpha_1\beta^2\frac{\partial^4\beta_\theta}{\partial\xi^2\partial\theta^2}$$
$$-\frac{2}{5}\alpha_1\beta^3\frac{\partial^4\beta_x}{\partial\xi\partial\theta^3}-\frac{2}{5}\alpha_1\beta^3\frac{\partial^4\beta_x}{\partial\xi\partial\theta^3}+\frac{8}{15}\alpha_1\beta\frac{\partial^4\beta_x}{\partial\xi^3\partial\theta}-16\frac{\alpha_1}{h^2}\frac{\partial^2\beta_\theta}{\partial\xi^2}-\frac{32}{5}\frac{\alpha_1\beta^2}{h^2}\frac{\partial^2\beta_\theta}{\partial\theta^2}+3\frac{Q_{44}}{h^2}\beta_\theta$$
$$-\alpha_2\beta^2\frac{\partial^4\beta_\theta}{\partial\xi^2\partial\theta^2}+\frac{2}{15}\alpha_1\beta\frac{\partial^4\beta_x}{\partial\xi^3\partial\theta}+\alpha_2\beta^2\frac{\partial^4\beta_\theta}{\partial\xi^2\partial\theta^2}+\frac{8}{15}\alpha_1\beta^2\frac{\partial^4\beta_\theta}{\partial\xi^2\partial\theta^2}+\frac{8}{15}\alpha_1\beta^3\frac{\partial^4\beta_x}{\partial\xi\partial\theta^3}+\frac{8}{15}\alpha_1\beta^3\frac{\partial^4\beta_x}{\partial\xi\partial\theta^3}$$
$$-\frac{2}{5}\alpha_1\beta\frac{\partial^4\beta_x}{\partial\xi^3\partial\theta}+2\alpha_0\beta^2\frac{\partial^4\beta_\theta}{\partial\xi^2\partial\theta^2}+\frac{4}{5}\alpha_1\beta^4\frac{\partial^4\beta_\theta}{\partial\theta^4}+\frac{16}{15}\alpha_1\beta^2\frac{\partial^4\beta_\theta}{\partial\xi^2\partial\theta^2}+2\alpha_0\beta^2\frac{\partial^4\beta_\theta}{\partial\xi^2\partial\theta^2}-\frac{1}{2}Q_{21}\beta\frac{\partial^2\beta_x}{\partial\xi\partial\theta}$$
$$-\frac{1}{4}Q_{66}\beta^2\frac{\partial^2\beta_x}{\partial\xi\partial\theta}-\frac{1}{2}\alpha_2\beta\frac{\partial^4\beta_x}{\partial\xi^3\partial\theta}-\frac{32}{15}\frac{\alpha_1}{h^2}\beta\frac{\partial^3 w}{\partial\xi^2\partial\theta}-\frac{1}{2}Q_{12}\beta\frac{\partial^2\beta_x}{\partial\xi\partial\theta}+15\frac{\alpha_2}{h^2}\beta\frac{\partial^3 w}{\partial\xi^2\partial\theta}-3\frac{\alpha_2\beta^3}{h^2}\frac{\partial^3 w}{\partial\theta^3} \quad (15e)$$
$$-\frac{24}{5}\frac{\alpha_1\beta^2}{h^2}\frac{\partial^2\beta_x}{\partial\xi\partial\theta}-24\frac{\alpha_0\beta}{h^2}\frac{\partial^2\beta_x}{\partial\xi\partial\theta}-\frac{1}{4}Q_{66}\beta^2\frac{\partial^2\beta_\theta}{\partial\xi^2}+\frac{1}{4}\alpha_2\frac{\partial^4\beta_\theta}{\partial\xi^4}+\frac{8}{15}\alpha_1\beta^2\frac{\partial^4\beta_\theta}{\partial\xi^2\partial\theta^2}+\frac{8}{15}\alpha_1\frac{\partial^4\beta_\theta}{\partial\xi^4}$$
$$+\frac{1}{4}\alpha_2\beta^2\frac{\partial^4\beta_\theta}{\partial\xi^2\partial\theta^2}-Q_{22}\beta^2\frac{\partial^2\beta_\theta}{\partial\theta^2}-\frac{32}{15}\frac{\alpha_1}{h^2}\beta^2\frac{\partial^2\beta_\theta}{\partial\theta^2}-\frac{24}{5}\frac{\alpha_1}{h^2}\beta\frac{\partial^2\beta_x}{\partial\xi\partial\theta}-\frac{64}{5}\frac{\alpha_1}{h^2}\beta^2\frac{\partial^2\beta_\theta}{\partial\theta^2}-8\frac{\alpha_1}{h^2}\beta\frac{\partial^3 w}{\partial\xi^2\partial\theta}$$
$$+\frac{8}{5}\frac{\alpha_1}{h^2}\beta\frac{\partial^3 w}{\partial\xi^2\partial\theta}-12\frac{\alpha_2}{h^2}\frac{\partial^2\beta_\theta}{\partial\xi^2}-3\frac{\alpha_2\beta^2}{h^2}\frac{\partial^2\beta_\theta}{\partial\theta^2}+9\frac{\alpha_2}{h^2}\beta\frac{\partial^2\beta_x}{\partial\xi\partial\theta}-24\frac{\alpha_0\beta^2}{h^2}\frac{\partial^2\beta_\theta}{\partial\theta^2}-12\frac{\alpha_2\beta}{h^2}\frac{\partial^3 w}{\partial\xi^2\partial\theta}$$
$$+6\frac{\alpha_2\beta^3}{h^2}\frac{\partial^3 w}{\partial\theta^3}-\frac{\partial^2\beta_\theta}{\partial\tau^2}=0$$

8 SOLUTION METHOD

Considering following form for the displacement fields, motion equations are simplified to one-dimensional equations as:

$$\begin{aligned}
u(x,\theta,t)&=U(x)\cos(m\theta)\,e^{\omega t},\\
v(x,\theta,t)&=V(x)\sin(m\theta)\,e^{\omega t},\\
w(x,\theta,t)&=W(x)\cos(m\theta)\,e^{\omega t},\\
\beta_x(x,\theta,t)&=\bar{\beta}_x(x)\cos(m\theta)\,e^{\omega t},\\
\beta_\theta(x,\theta,t)&=\bar{\beta}_\theta(x)\sin(m\theta)\,e^{\omega t},
\end{aligned} \quad (16)$$

where ω (*rad/s*) is the natural circular frequency of the cylindrical shell and m is integer number which introduced as circumferential wave numbers.

After this simplifying, one dimensional DQM is used to approximate the partial derivative of function. Let F be a function representing u, w, v, β_x and β_θ with respect to variables ξ in the domain of ($0<\xi<L$) [27]:

$$\frac{\partial^k F}{\partial\zeta^k}=\sum_{k=1}^{N}A_{pq}^{(K)}F(\zeta_i), \quad (17)$$

where $A_{pq}^{(k)}$ is the weighting coefficients associated with k^{th}-order partial derivative of *F*, and *N* is the number of grid points in longitudinal direction. Chebyshev polynomials [27] are selected for positions of the grid points. Substituting Eq. (16) to Eqs. (15) and using Eq. (17) algebraic equations are achieved as follows:

$$M\ddot{Y} + C\dot{Y} + KY = 0, \tag{18}$$

where *Y* is the displacement vector, *M* is the mass matrix, *C* is the damping matrix and *K* is the stiffness matrix.

Applying simply-simply boundary conditions into the final equations, the standard form of motion equations is obtained. Dimensionless frequencies are the eigen-value of following matrix ([*A*]) that are named state-space matrix:

$$[\mathrm{A}] = \begin{bmatrix} [0] & [\mathrm{I}] \\ -[\mathrm{M}^{-1}\mathrm{K}] & -[\mathrm{M}^{-1}\mathrm{C}] \end{bmatrix}, \tag{19}$$

where [*I*] and [0] are the unitary and zero matrixes. Results of Eq. (19) are complex values that contain real (damping frequencies) and imaginary (natural frequencies).

9 NUMERICAL AND DISCUSSION

In this research, vibrational behavior of orthotropic protein MTs in living cells is investigated using Cooper-Naghdi shell model. The effect of various parameters such as length scale, length to radius ratio, thickness of MT, surface layer and temperature change in living cells are discussed in details. Mechanical properties of orthotropic MT are expressed in Table 1.

Table 1
Mechanical properties of MTs.

h	R_2	β	E_x	E_θ	γ
2.7e-9 *nm*	12.8e-9 *nm*	40	1e9 *Pa*	1e6 *Pa*	0.0001
$l_0 = l_1 = l_2$	υ_x	k	E_c	ρ_m	μ
10e-5 *nm*	0.3	5/6	1e3 *Pa*	1470 *kg/m*^{3}	695e-6 *Pa.s*

The longitudinal elastic modulus of MTs is significantly greater than shear modulus and the circumferential elastic modulus. For this reason, the effect of longitudinal Young's modulus on vibration frequencies of anisotropic MTs is demonstrated in Fig. 2. This figure reveals that the natural frequency of anisotropic MT enhances due to increasing the stiffness of MTs with increasing the longitudinal Young's modulus as it has also been concluded in Ref. [8].

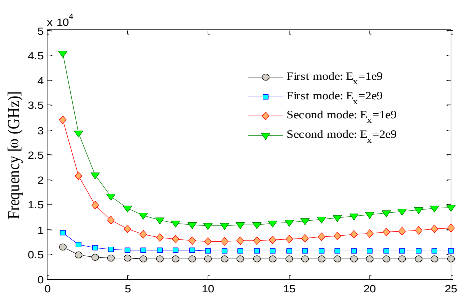

Fig.2
Variation of vibration frequency with circumferential wave numbers for different values of Young's modulus.

MTs are cylindrical structures with inner and outer diameters of about 17 and 25 nm, respectively. Therefore, it's better to simulate anisotropic MT as thick shell model. In this regard, vibration frequencies of anisotropic MT versus circumferential wave numbers for different MT thickness-effective thickness for bending (h_0) and equivalent thickness (h) [12] are illustrated in Fig. 3. It is obvious from this figure that decreasing the thickness of MT leads to increase natural vibration frequencies. It is worth to mention that the thickness of MT is a key parameter especially for higher vibration modes and lower circumferential wave numbers.

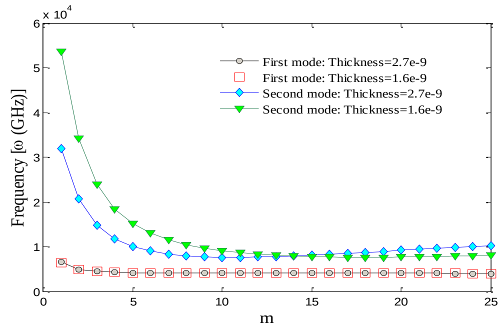

Fig.3
Effect of thickness of MT on vibration frequency versus circumferential wave numbers.

Fig. 4 shows the effect of length to radius ratio on vibration frequencies of anisotropic MT. It is obvious that the stiffness of protein MT with smaller aspect ratio is substantial, so that, decreasing the value of aspect ratio from 50 to 45, leads to increase natural frequencies considerably (about 1800 *GHZ*). This result has also been obtained in Refs. [12] and [23]

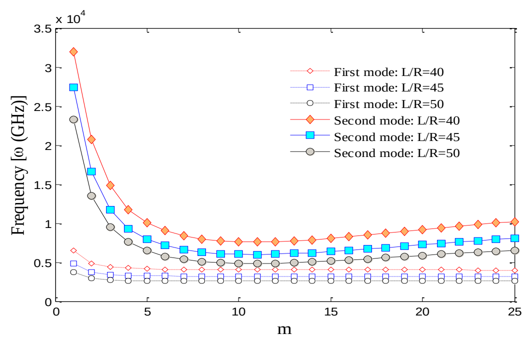

Fig.4
Vibration frequency of MTs for different length to radius ratios.

Effect of temperature change in living cells on the vibrational behavior of protein MT is depicted in Fig. 5. The mechanical properties of anisotropic MT are expressed in Table 2. This figure shows that increasing temperature in the living cell tissues causes to decrease frequencies of anisotropic protein MT extraordinary.

Table 2
Temperature-dependent material properties for microtubules.

	E_x	E_θ	$G_{x\theta} = G_{xz} = G_{\theta z}$
$T = 15\,^\circ C$	185e6 *Pa*	1.47e6 *Pa*	1.9e6 *Pa*
$T = 20\,^\circ C$	138e6 *Pa*	1.09e6 *Pa*	1.5e6 *Pa*
$T = 30\,^\circ C$	127e6 *Pa*	1e6 *Pa*	1.3e6 *Pa*

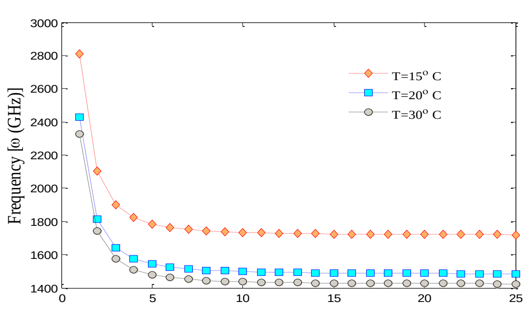

Fig.5
Effect of temperature in living cells on vibration frequency of MT.

Fig. 6 represents effect of surface layer on frequencies of protein MT. This figure indicates that considering surface layer around the MT does not effect on vibrational behavior of MT significantly. But it should be considered to enhance the accuracy of results; also some conditions may increase the effect of surface layer such as initial axial compression loading as it has been investigated in Ref. [26]

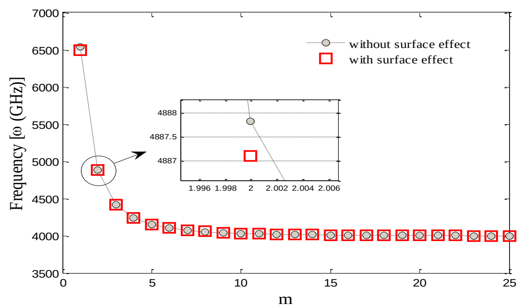

Fig.6
Effect of surface layer of MT on vibration frequency.

Fig. 7 indicates the comparison between the results of classic, couple stress and strain gradient theories. As can be seen, due to considering three length scale parameter in strain gradient theory, the difference in the frequencies of MT that predicted by this theory compared with couple stress and classical theory is significant. This difference expresses the superiority and accuracy of strain gradient theory than other theories like the results obtained from Ref. [28].

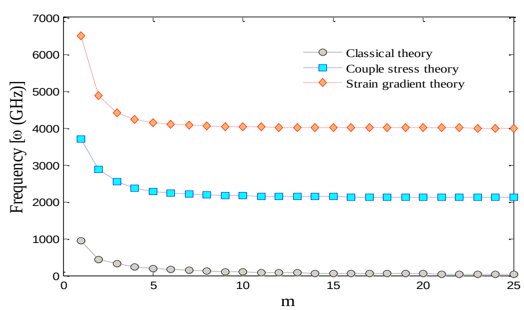

Fig.7
Comparison between the results of classic, couple stress and strain gradient theories.

As mentioned already, strain gradient theory involves three length scale parameters. Fig. 8 illustrates the effect of three length scale parameters on natural frequency (*Hz*), separately. As can be seen from this figure, the most value of frequency is belong to l_1 , while l_0 needs larger value to change the natural frequency. Figs. 8(a) and 8(b) show when l_1 increases the natural frequency from $3.92e8(Hz)$ *to* $2.51e9(Hz)$, l_0 changes it only from $3.92e8(Hz)$ *to* $4.19e8(Hz)$ which is very negligible. In the other hand, the increasing rate of l_1, l_2 is greater than l_0 .Increasing every three parameters, the frequency increases like the findings of Ref. [28]. The results approved that l_0, l_1, l_2 have significant effect on vibrational behavior of MTs and strain gradient theory can apply the effect of size in microstructures, as well.

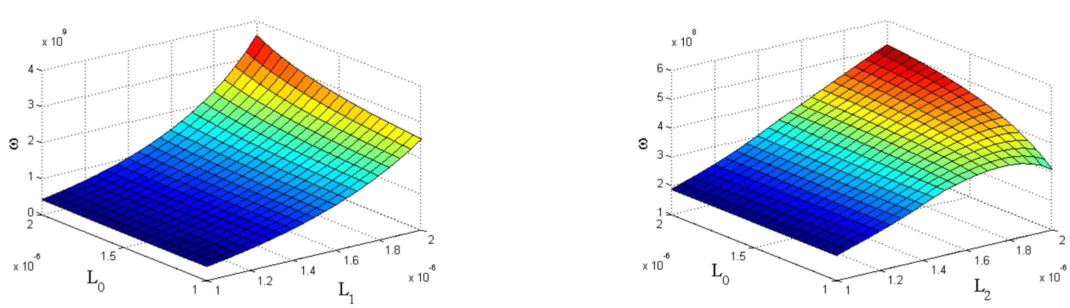

(a) (b)

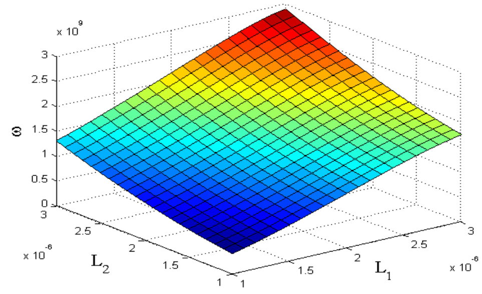

(c)

Fig.8
Vibration frequency versus length scale parameters (a) l_2 is 0.5 micrometer. (b) l_1 is 0.5 micrometer. (c) l_0 is 15 micrometer.

In order to validate the results, equations of motion were solved by the shell theory presented in Ref. [16]. The results of Cooper-Naghdi shell theory and Heireche et al. [16] have been compared in Fig. 9. As can be seen in Fig. 9, there is a good agreement between the result of these theories especially in $m = 1, 9, 10$. This figure approved the accuracy of Cooper–Naghdi thick shell theory.

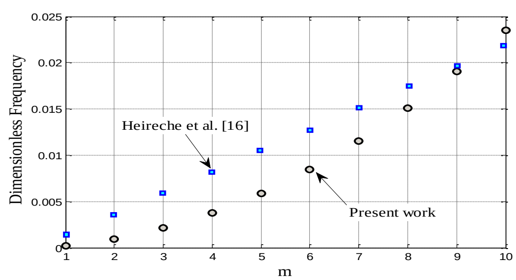

Fig.9
Comparison between the results of present work and Ref. [16].

10 CONCLUSIONS

This study has been developed strain gradient theory using Cooper–Naghdi thick shell model for the first time. Vibrational behavior of anisotropic protein MTs surrounded in cytosol was investigated with the new approach. Cytosol was considered as a visco-elastic bio-medium and the influence of surface traction are also taken into account. The effect of three length scale parameters on vibration frequency of anisotropic MT was determined. The governing motion equations were obtained using Hamilton's principle and solved by one dimensional DQ method for simply- simply boundary condition. Regarding thermo-mechanical properties of MT, effect of various parameters such as temperature change, length scale, surface layer, thickness and aspect ratio on the frequencies of anisotropic MT were discussed in details and following results were concluded:

- The results approved that temperature in living tissues and physical properties of MT such as longitudinal elastic modulus, thickness and aspect ratio play an important role on vibration frequencies of MT, so that increasing temperature in the living cell tissues causes to decrease frequencies of anisotropic protein MT extraordinary.
- It is obvious that the stiffness of protein MT with smaller aspect ratio is substantial, so that, decreasing the value of aspect ratio from 50 to 45, leads to increase natural frequencies considerably (about 1800 *GHZ*).
- Decreasing the thickness of MT leads to increase natural vibration frequencies.
- It was found that vibrational behavior of MT is strongly dependent on the length scale parameter so that increasing length scale significantly increased the frequency especially for higher vibration modes.
- Considering surface layer around the MT does not effect on vibrational behavior of MT significantly. But it should be considered to enhance the accuracy of results; also some conditions may increase the effect of surface layer such as initial axial compression loading.

ACKNOWLEDGEMENTS

We would like to thank the referees for their valuable comments.

REFERENCES

[1] Cooper G.M., Hausman R.E., 2007, *The Cell: A Molecular Approach*, ASM Press, Washington.

[2] Shi Y.J., Guo W.L., Ru C.Q., 2008, Relevance of Timoshenko-beam model to microtubules of low shear modulus, *Physica E* **41**: 213-219.

[3] Gao Y., Lei F.M., 2009, Small scale effects on the mechanical behaviors of protein microtubules based on the nonlocal elasticity theory, *Biochemical and Biophysical Research Communications* **387**: 467-471.

[4] Tounsi A., Heireche H., Benhassaini H., Missouri M., 2010, Vibration and length-dependent flexural rigidity of protein microtubules using higher order shear deformation theory, *The Journal of Theoretical Biology* **266**: 250-255.

[5] Fu Y., Zhang J., 2010, Modeling and analysis of microtubules based on a modified couple stress theory, *Physica E* **42**: 1741-1745.

[6] Civalek O., Demir C., 2011, Bending analysis of microtubules using nonlocal Euler–Bernoulli beam theory, *Applied Mathematical Modelling* **35**: 2053-2067.

[7] Demir Ç., Civalek Ö., 2013, Torsional and longitudinal frequency and wave response of microtubules based on the nonlocal continuum and nonlocal discrete models, *Applied Mathematical Modelling* **37**: 9355-9367.

[8] Cooper R.M., Naghdi P.M., 1957, Propagation of non-axially symmetric waves in elastic cylindrical shells, *Journal of the Acoustical Society of America* **29**: 1365-1372.

[9] Daneshmand F., Ghavanloo E., Amabili M., 2011, Wave propagation in protein microtubules modeled as orthotropic elastic shells including transverse shear deformations, *Journal of Biomechanics* 44: 1960-1966.

[10] Gao Y., An L., 2010, A nonlocal elastic anisotropic shell model for microtubule buckling behaviors in cytoplasm, *Physica E* **42**: 2406-2415.

[11] Gheshlaghi B., Hasheminejad S.M., 2011, Surface effects on nonlinear free vibration of nano-beams, *Composites: Part B* **42**: 934-937.

[12] Ghorbanpour Arani A., Kolahchi R., Khoddami Maraghi Z., 2013, Nonlinear vibration and instability of embedded double-walled boron nitride nano-tubes based on nonlocal cylindrical shell theory, *Applied Mathematical Modelling* **37**: 7685-7707.

[13] Ghorbanpour Arani A., Shajari A.R., Amir S., Loghman A., 2012, Electro-thermo-mechanical nonlinear nonlocal vibration and instability of embedded micro-tube reinforced by BNNT, *Physica E* **45**: 109-121.

[14] Ghorbanpour Arani A., Shirali A.A., Noudeh Farahani M., Amir S., Loghman A., 2012, Nonlinear vibration analysis of protein microtubules in cytosol conveying fluid based on nonlocal elasticity theory using differential quadrature method, *Proceedings of the Institution of Mechanical Engineers, Part C: Journal of Mechanical Engineering Science* **227**: 137-145.

[15] Gu B., Mai Y. W., Ru C. Q., 2009, Mechanics of microtubules modeled as orthotropic elastic shells with transverse shearing, *Acta Mechanica* **207**: 195-209.

[16] Heireche H., Tounsi A., Benhassaini H., Benzair A., Bendahmane M., Missouri M., Mokadem S., 2010, Nonlocal elasticity effect on vibration characteristics of protein microtubules, *Physica E* **42**: 2375-2379.

[17] Karimi Zeverdejani M., Tadi Beni Y., 2013, The nano scale vibration of protein microtubules based on modified strain gradient theory, *Current Applied Physics* **13**: 1566-1576.

[18] Liew K.M., Wang Q., 2007, Analysis of wave propagation in carbon nanotubes via elastic shell theories, *International Journal of Engineering Science* 45: 227-241.

[19] Shen H.S., 2013, Nonlocal shear deformable shell model for torsional buckling and postbuckling of microtubules in thermal environments, *Mechanics Research Communications* **54**: 83- 95.

[20] Shu C., 2000, *Differential Quadrature and its Application in Engineering*, Springer, London.

[21] Taj M., Zhang J., 2014, Analysis of wave propagation in orthotropic microtubules embedded within elastic medium by Pasternak model, *Journal of the Mechanical Behavior of Biomedical Materials* **30**: 300-305.

[22] Taj M., Zhang J.Q., 2012. Analysis of vibrational behaviors of microtubules embedded within elastic medium by Pasternak model, *Biochemical and Biophysical Research Communications* **424**: 89-93.

[23] Wang C.Y., Li C.F., Adhikari S., 2009, Dynamic behaviors of microtubules in cytosol, *Journal of Biomechanics* **42**: 1270-1274.

[24] Wang C.Y., Ru C.Q., Mioduchowski A., 2006, Vibration of microtubules as orthotropic elastic shells, *Physica E* **35**: 48-56.

[25] Wang C.Y., Zhang L.C., 2008, Circumferential vibration of microtubules with long axial wavelength, *Journal of Biomechanics* **41**: 1892-1896.

[26] Wang L., 2010, Vibration analysis of fluid-conveying nanotubes with consideration of surface effects, *Physica E* **43**: 437-439.

[27] Wang X., Yang W.D., Xiong J.T., 2014, Coupling effects of initial stress and scale characteristics on the dynamic behavior of bio-liquid-filled microtubules immersed in cytosol, *Physica E* **56**: 342-347.

[28] Zhou X., Wang L., 2012, Vibration and stability of micro-scale cylindrical shells conveying fluid based on modified couple stress theory, *Micro & Nano Letters* **7**: 679-684.